Reciprocal Relations in Glass-Making and Bond-Breaking Components in the Chemical Composition of Mould Powders

A.R. Arefpour*[1], S. Jabbarzare[2], A. Monshi[3], A. Saidi[4]

Advanced Materials Research Center, Department of Materials Engineering, Najafabad Branch, Islamic Azad University, Najafabad, Iran

Abstract

Mould powders are mainly composed of SiO_2, CaO, alkaline, and alkaline-earth oxides along with traces of fluoride and carbon. Their crucial responsibility is lubricating the surface between mould walls and the solidified steel crust. The viscosity and crystallization of the powders are influenced by fluorine. However, the emission of evaporating materials leads to environmental pollution. The research aims to reduce values of CaF_2 and the effect of substitute compositions on the viscosity and crystallization of mould powders. Therefore, 12 powder samples are prepared having employed Portland Cement Clinker and others as the main composition. To compare the laboratory samples with the molten reference powder, groove viscometer tests were conducted. The crystalline behavior of the samples was examined employing XRD, SEM and STA analyses. Results showed that some low-CaF_2 samples possessed proper viscosity as molten reference powder (MRP). XRD analysis results presented crystalline phases of gehlenite, cuspidine, akermanite, nepheline and Mn_3O_4. Likewise, the crystalline phases of B_2SiO_5, Na_2ZnSiO_4 and perovskite ($CaTiO_3$) were examined after adding B_2O_3, ZnO and TiO_2. SEM analysis results showed that crystals in the glass matrix, which can optimize the viscosity in mould powders. TGA analysis results revealed that the reduction on ignition loss of a low-CaF_2 sample compared to the reference powder. Moreover, DTA analysis revealed the crystallization and melting temperatures of the same low-CaF_2 sample, similar to that of the reference powder. It can be concluded that three low-CaF_2 samples containing CaF_2, Li_2O, TiO_2, ZnO and B_2O_3 were nominated as the apt substitutions for reference powder in laboratory scale.

Keywords: Crystallization, Mould Powder(MP), Molten Reference Powder (MRP), Portland Cement Clinker, Titanium Oxide, Viscosity, Zinc Oxide.

1. Introduction

Mould powders are applied in steel industries as raw materials are mainly composed of SiO_2, CaO, Al_2O_3, alkaline and alkaline-earth oxides along with traces amounts of fluoride and carbon. The powders, mainly used in continuous casting of steel slabs, play a crucial role in the consistency of the process and final surface quality of the products [1-3].

Selecting the type and properties of the powders mainly depends on factors such as type of steel, casting temperature, casting speed and mould dimensions.

Such powders principally possess function such as protecting the molten metal's surface from oxidation, preventing the heat loss and local solidification in some surface points (Thermal insulation), lubricating, absorption the inclusions, controlling the heat transfer between

*Corresponding author
Email: arefpour.a@gmail.com
Address: Advanced Materials Research Center, Department of Materials Engineering, Najafabad Branch, Islamic Azad University, Najafabad, Iran
1.PhD
2. Instructor
3. Professor
4. Professor

the crust and the mould via the solidified crust and decreasing the intensity of oscillatory signs [4-8].

In recent years, dispersion of toxic materials from powders including fluorine (CaF_2) in cooling waters and its deleterious effects on the environment has been one of the considerably concerning issues which led the studies toward substituting the CaF_2 with other harmless substances. In addition, the emission of toxic compounds containing CaF_2 like HF, SiF_4, NaF, etc. has been one of the greatest issues in the environmental studies since these compounds are dissolved in cooling waters and make it acidified. The phenomenon leads to the erosion and corrosion of industrial equipment, the poisoning of water and soil followed by jeopardizing the immunity and health in the environment [9-11]. Due to technical particularities such as decreasing the melting temperature and viscosity as well as producing crystal particles, CaF_2 is extensively deployed in the slag film. Therefore, any substitute material should meet these objectives [9]. Mould powders comprise of other components whose tasks are as follows:

A. Alkaline oxides: These mainly consisted of sodium and potassium oxides (Na_2O and K_2O). They tend to decrease the melting point and surface tension of the slag[12].

B. Alkaline–earth oxides: The most important of such are magnesium and calcium oxides (MgO and CaO). The CaO's crucial task is to adjust the basicity. Basicity directly influences the viscosity, crystallization temperature and the ability to absorb inclusions. Basicity value might vary between 0.6-1.4 [13, 14].

C. Silica and Alumina (SiO_2 and Al_2O_3): These two substances enhance the viscosity. The most crucial duty of SiO_2, however, is to produce molten silicate. Metallic oxides like Na_2O, K_2O, CaO, and Fe_2O_3 are present in sufficient quantities adjacent to SiO_2 which constitute the main structure of silicates composed of SiO^{-4}_4 tetrahedrons. Thus, molten silicates construct a continuous network and can cover the molten surface. Similar to SiO_2, Al_2O_3 is a network-making substance that reduces the crystallization of the molten slag [15, 16].

D. Iron oxide (Fe_2O_3) as well as manganese oxide (MnO) are the lubricants [17]. The chemical composition of mould powder is highly effective on the viscosity. Compounds present in mould powders can be divided into two main categories: The first group is network-making substances which constitute a molten lattice structure such as SiO_2 and Al_2O_3. The second group are bond-breaking compounds which cause the viscosity and lubrication of the slag to diminish by breaking the bonds. They generally include the oxides such as Na_2O, K_2O, Li_2O, CaO, MgO, MnO, Fe_2O_3, B_2O_3, and the bond-breaking substance which is CaF_2. The effect of some of the compounds such as titanium oxide (TiO_2) on the viscosity is highly complex; for instance, addition of 6wt% of TiO_2 to the mould powder reduces the viscosity while in higher amounts the viscosity value drops down. The fact shows that TiO_2 in amounts less than 6wt% acts as a bond-breaking substance and by breaking the bonds in the network structure decreases the viscosity. In higher amounts, however, by entering the network structure functions as a network-making component and accordingly, increments the viscosity [9]. Therefore, the addition of Al_2O_3 and SiO_2 raise the viscosity, where Li_2O and Na_2O leads to its reduction. Thus the ratio of these oxides called glass ratio is presented in relation No. 1:

$$\text{Glass ratio} = \frac{Na_2O + Li_2O}{Al_2O_3 + SiO_2} \qquad \text{Eq. (1)}$$

In which the higher the ratio, the lower the viscosity [4].

The objective of the research is to study the effect of altering the mould powder composition used in the continuous high speed casting industry. In addition, the study aims at modifying the chemical composition of high lubricating powder and to prepare combinations with the aim of cutting down on CaF_2 by its removing or substituting within powder's chemical composition. And finally, to examine the effect of substituting components on the viscosity and crystallization of these powders. To achieve the goal, components such as CaF_2 and the oxides such as ZnO, Na_2O, B_2O_3, Ti_2O, Li_2O, K_2O and MgO were applied as raw materials in the prepared powders. Then, their viscosity as well as their crystalline behavior was studied. They were compared with the molten reference powder and accordingly, the optimum compounds were introduced.

2. Materials and methods

2.1. Raw materials

The mould lubricant powder (reference powder) was identified whose chemical composition is presented in Table 1.

The powder was selected as the reference powder having been identified and was attempted to develop compounds through changing the chemical composition of the substance regarding its specifications. Portland cement clinker, silica (SiO_2), sodium carbonate (Na_2CO_3), calcium fluorine (CaF_2), zinc oxide (ZnO), magnesium oxide (MgO), titanium oxide (Ti_2O), lithium oxide (Li_2O), bohr oxide (B_2O_3), potassium oxide (K_2O) and manganese oxide (MnO) were applies as raw materials. It is worth mentioning that in the research Portland cement clinker type I (Table 2) due to its very low sulphur content was utilized as the main compound (base compound) to make the powders.

Table 1. The chemical composition of the reference powder based on weight percentage.

Chemical composition	Weight percentage
LOI	15- 18
$C_{(total)}$	7-9
$C_{(free)}$	4.5 – 6.5
SiO_2	28 – 29.5
Fe_2O_3	1 – 2.5
Al_2O_3	3 – 5
CaO	26 – 28
MgO	5 – 6
$Na_2O + K_2O$	6 – 8
MnO	4 – 6
F^-	3 – 4
S	< 0.3
H_2O (120 ℃)	< 0.8

Table 2. The chemical composition of Portland Cement Clinker Type I based on weight percentage.

Chemical composition	Weight percentage
SiO_2	21.78
Al_2O_3	5.41
Fe_2O_3	3.14
CaO	64.32
MgO	1.89
K_2O	0.73
Na_2O	0.28
SO_3	0.01

2.2. Test procedures

2.2.1. Decarburization of the reference powder

Carbon is used in the chemical composition of mould powders to control melting speed [4, 18]. On the other hand, carbon is by no means involved in controlling the viscosity because it burns and causes heat loss. Therefore, the reference powder was decarburized for 12 hours at 750 °C [19].

2.2.2. Preparation of Powders

With respect to chemical analysis of the reference powder (Table 1), chemical analysis of the decarburized reference powder obtained from XRF analysis (Table 3) and basicity of this powder (CaO/SiO_2=0.94) and also considering the chemical composition of the Portland cement clinker (Table 2), in this research, 12 powder samples via the aforementioned raw materials were prepared.

Table 3. The chemical composition of the decarburized reference powder obtained from XRF analysis based on weight percentage.

Chemical composition	Weight percentage
CaO	35.99
SiO_2	31.06
Na_2O	8.78
MnO	5.95
Al_2O_3	5.59
MgO	5.58
F^-	4.50
Fe_2O_3	2.67
SO_3	0.387
TiO_2	0.275
K_2O	0.199
LOI*	0.63

Chemical composition of the powders based on

weight of the raw materials (gram) and based on weight percentage are presented in Tables 4 and 5, respectively. First, raw materials were mixed with specified ratios according to Table 4. To homogenize the powders, laboratory samples along with ethanol (96% pure) of the same weight as each sample were prepared in the ball mill with a speed of 600 Rpm for 5 min. It is worth mentioning that in the stage, some parameters such as the number of balls and the mill rotation speed for all the samples were constant. Afterwards, to evaporate ethanol and dry up the prepared powders, the samples were put into oven with a temperature of 110°C for 3 h so as to become fully dry.

2.2.3. Comparison of Viscosity

To obtain a comparison between the viscosity of samples in real conditions without using mathematical relations and in a practical way, the groove viscometer test was employed which studies the viscosity of powders in a comparative manner. The viscometer is a porcelain disc with depressed grooves, and the samples were placed as pellets above the depressions. The viscometer along with the samples were placed at a 45° furnace. Following heating, the height of the molten flown in these grooves was compared with the height of MRP absorbed in grooves of the viscometer. To do this test, one-gram samples of the prepared powders and the reference powder under a 6 ton press were changed into pellets with a height of 1.5mm and a diameter of 13mm and were placed in the upper part of these viscometers.

After that, the whole set (viscometer along with prepared pellets of samples and the reference powder) were heated in the furnace up to 1150°C so that their molten viscosity in the conditions can be compared with each other.

Table 4. The chemical composition of laboratory samples based on gram.

	CaO	SiO_2	Al_2O_3	Fe_2O_3	MnO	MgO	Na_2O	F^-	K_2O	TiO_2	Li_2O	ZnO	C	B_2O_3	S
V_1	32.3	31.23	2.47	1.43	5.95	9.58	8.63	2	0.33				1.64		0.004
V_2	30.83	31.23	2.47	1.43	5.95	10.58	8.63	1	0.33				1.64		0.004
V_3	29.36	31.23	2.47	1.43	5.95	11.58	8.63		0.33				1.64		0.004
T_7	32.3	31.23	2.47	1.43	5.95	5.58	8.63	2	0.33		0.2		1.72		0.004
T_8	30.83	31.23	2.47	1.43	5.95	5.58	8.63	1	0.33		0.4		1.8		0.004
T_9	29.36	31.23	2.47	1.43	5.95	5.58	8.63		0.33		0.8		1.96		0.004
U_1	32.3	31.23	2.47	1.43	5.95	5.58	8.63	2	4.33				1.64		0.004
U_2	30.83	31.23	2.47	1.43	5.95	5.58	8.63	1	5.33				1.64		0.004
U_3	29.36	31.23	2.47	1.43	5.95	5.58	8.63		6.33				1.64		0.004
S_1	30.83	31.23	2.47	1.43	5.95	5.58	8.63	1	1.33	5	0.4		1.8		0.004
S_2	30.83	31.23	2.47	1.43	5.95	5.58	8.63	1	0.33	5		2	1.64		0.004
S_3	30.83	31.23	2.47	1.43	5.95	5.58	8.63	1	0.33	5			1.64	2	0.004

Table 5. The chemical composition of laboratory samples based on weight percentage

	CaO	SiO_2	Al_2O_3	Fe_2O_3	MnO	MgO	Na_2O	F^-	K_2O	TiO_2	Li_2O	ZnO	C	B_2O_3	S
V_1	33.8	32.7	2.6	1.5	6.23	10.02	9.03	2.09	0.34				1.72		0.004
V_2	32.76	33.2	2.62	1.52	6.32	11.24	9.17	1.06	0.35				1.74		0.004
V_3	31.7	33.72	2.67	1.54	6.42	12.5	9.32		0.36				1.77		0.004
T_7	35.2	34	2.7	1.56	6.5	6.07	9.4	2.2	0.36		0.22		1.87		0.004
T_8	34.4	34.83	2.75	1.6	6.64	6.22	9.62	1.11	0.37		0.45		2		0.004
T_9	33.46	35.6	2.81	1.63	6.78	6.36	9.83		0.38		0.9		2.23		0.004
U_1	33.8	32.7	2.6	1.5	6.23	5.84	9.03	2.09	4.53				1.72		0.004
U_2	32.76	33.19	2.62	1.52	6.32	5.93	9.17	1.06	5.66				1.74		0.004
U_3	31.7	33.72	2.67	1.54	6.42	6.02	9.32		6.83				1.77		0.004
S_1	32.23	32.65	2.58	1.49	6.22	5.83	9.02	1.04	1.39	5.23	0.42		1.88		0.004
S_2	32.08	32.5	2.57	1.5	6.19	5.81	8.98	1.04	0.34	5.2		2.08	1.71		0.004
S_3	32.08	32.5	2.57	1.5	6.19	5.81	8.98	1.04	0.34	5.2			1.71	2.08	0.004

2.2.4. Studying Crystalline Behavior

XRD patterns (Philips device PW3040) were applied to identify the phases present in the reference powder as well as to study the crystalline phases developed in the selected molten samples on the viscometer grooves and compare them with the employed crystalline phases of molten reference powders (MRP). SEM images (VEGA-TESCAN, Czech Republic were applied to investigate the microstructure of the selected samples. Finally, to study the melting and crystallization temperatures of the reference powder and the selected samples, the STA graph (STA 503, USA) was employed.

3. Results and discussion

3.1. Studying the effect of viscosity

3.1.1. Studying the effect of MgO on the viscosity of low-CaF_2 and CaF_2-free samples containing Portland Cement Clinker

Sample V_1 contained 2.09wt% CaF_2 (4.1g CaF_2) and the amount of MgO in the sample was 10.02wt% evidently, the primary amount of MgO in sample V_1 composition regarding the formulation of the reference powder was 5.84wt% and the amount has been increased to 10.02wt%. It is true for samples V_2 and V_3. Sample V_2 contained 1.06wt% CaF_2 (2.05 g CaF_2) and the amount of MgO from 5.93wt% was increased to 11.24wt%. In sample V_3 CaF_2 was completely removed from the sample and the MgO was increased from 6.02wt% to 12.5wt%. As depicted in Fig.1, the samples have gained no lubrication potential. By increasing the level of MgO instead of CaF_2, viscosity of the samples increases, which is clearly shown by the groove viscometer (Fig.1). CaF_2 is a lubricant compound which reduces viscosity; however, MgO is a refractory substance with a melting point of 2800°C which enhances the viscosity.

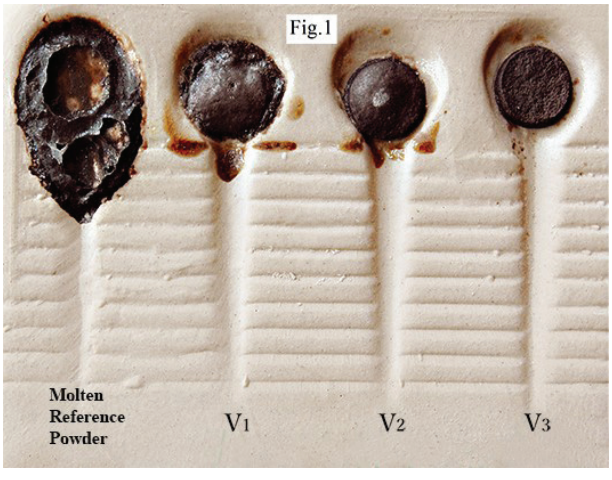

Fig.1. Schematic of molten samples of reference powder, V_1, V_2 and V_3 on the grooves of the groove viscometer.

It is assumed that the following reaction has happened in samples V_1, V_2 and V_3 (Eq. 2).

$$2Na_2O + SiO_2 \rightarrow Na^{1+}{}_4 + SiO^{4-}{}_4 \rightarrow \text{Glass} \qquad \text{Eq. (2)}$$

Now the presence of Mg^{2+} can conduct the rest of the reaction as follows (Eq. 3):

$$2Mg + SiO_2 \rightarrow 2Mg^{2+} + SiO^{4-}{}_4 \rightarrow Mg_2\,SiO_4\ (\text{forsterite}) \qquad \text{Eq. (3)}$$

Forsterite with a melting point of 1890°C forces mould powder's fluidity to decline and its viscosity to enlarge. Regarding Fig.2, CaF_2 with a melting point of 1390°C along with MgO with a melting point of 2800°C develops eutectic in 1350°C [3]. In the temperatures above 1350°C the evidence of melting begins to appear. Lack of CaF_2 raises the melting point and decreases fluidity since it does not develop eutectic. Fig.2 displays the fact. In other words, CaF_2 and MgO do not dissolve in each other, and develop eutectic in 1350°C. Existence of CaF_2 beside the MgO with a melting point of 2800°C raise the eutectic to around 1350°C and creates a eutectic point [3]. In addition, small amounts of CaF_2 alongside MgO similarly are capable of developing a mushy zone (Fig.2). The reason for insolubility of CaF_2 in MgO lies in the structure of CaF_2, in which Ca atoms are located in a position similar to that of the FCC structure and they have a tetrahedral structure in which they settled on the diameter, at a distance of 1/4 from the apex. MgO, however, has a structure similar to that of NaCl where oxygen is located in a position like FCC structure and Mg is situated on an octahedral location on the side. Displacement of a Ca ion from a FCC structure in CaF_2 to the octahedral location in the MgO structure is impossible.

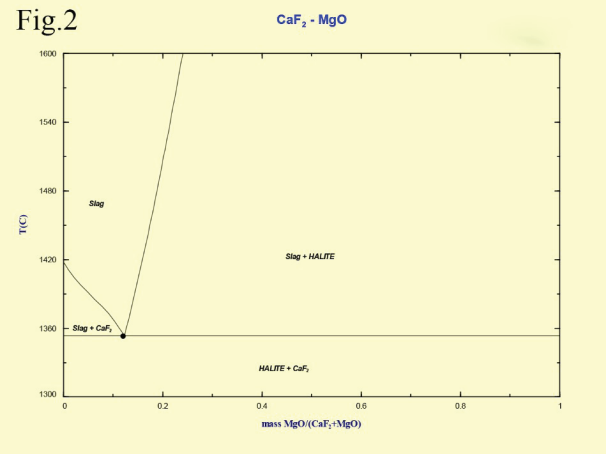

Fig.2. Diagram of CaF2-MgO[3].

In CaF_2 structure, each Ca ion is surrounded by 8 F^-

ions. Therefore, it leads to the reduction of free energy emission. In MgO, a coordination number of 6 has been sustained for Mg. The difference in coordination number is another obstacle for any displacement of Ca in the MgO structure.

Regarding the above-mentioned reasoning, it can be concluded that MgO is not the solely suitable substitute for CaF_2 in the chemical composition of the mould powder.

3.1.2. Studying the effect of Li_2CO_3 in low-CaF_2 and CaF_2-free samples including Portland Cement Clinker

The effect of Li_2CO_3 was examined in samples T_7, T_8 and T_9. Sample T_7 contained 2.2wt% CaF_2 (4.1g CaF_2) and 0.22wt% Li_2O (0.5g Li_2CO_3). Regarding Fig.3, it is observed that thanks to the addition of 0.5g Li_2CO_3, a suitable viscosity was obtained compared to that of the reference powder. Due to the heating process, Li_2CO_3 is decomposed to Li_2O and CO_2. Li_2O can penetrate into various oxides because the Li^+ ion is very small and, practically, has only the K electronic orbit. This penetration ability along with 2.2wt% CaF_2 shows a viscosity at the same level of the molten reference powder (Fig.3). Sample T_8 contained 1.11wt% CaF_2 (2.05g CaF_2) and 0.45wt% Li_2O (1g Li_2CO_3). By increasing Li_2CO_3 and reducing CaF_2, the viscosity of sample T8 is raised, compared to molten reference powder (Fig.3). Sample T_9 contained 0.9wt% Li_2O (2g Li_2CO_3) which was completely substituting CaF_2. When ccompared to molten reference powder (MRP), the viscosity of sample T_9 was highly increased by full omission of CaF_2 and increasing Li_2CO_3 (Fig.3). By lessening the amount of CaF_2 as lubricant and increasing Li_2CO_3 levels in samples T_8 and T_9, the viscosity grows. The event happens due to the fact that CaF_2 is stronger in breaking the bonds and developing CaF_2 compared with Li_2CO_3. With regard to relation 4, in Li_2SiO_4 formation, on condition that Li_2CO_3 substitutes for CaF_2, the potential to develop the eutectic point with a low melting point will be achieved. Under such conditions, the fluidity power of Li_2CO_3 is less than CaF_2. Consequently, it causes the reduction in fluidity of samples T_8 and T_9 as well as causing their viscosity to enhance. It can be concluded that employment of Li_2O in the amounts less than 0.22wt% in the chemical composition of the mould powder (MP) acts as a bond breaking factor and therefore, forces the viscosity of the MP to diminish. On the contrary, the application of Li_2O at levels higher than 0.22wt% in the chemical composition of the MP acts as a glass-making factor and compels the viscosity to enlarge. (Relation 4).

$$2Li_2O+SiO_2 \rightarrow Li^+_4 + SiO^{4-}_4 \rightarrow Li_2SiO_4 \qquad \text{Eq. (4)}$$

3.1.3. Studying the effect of K_2O on low-CaF_2 and CaF_2-free samples including Portland Cement Clinker

The group of samples, substituting F^- for K_2O in the samples'composition was carefully examined. The amount of K_2O present in samples U_1, U_2 and U_3 is 0.33g which exists in the chemical composition of the Portland cement clinker.

Sample U_1 contains 4.18wt% K_2O (4g K_2O) surplus to its existing K_2O and 2.09wt% F^- (4.1g CaF_2). Sample U_2 contains 5.31wt% K_2O (5g K_2O) surplus to the composition and 1.06wt% F^- (2.05g CaF_2). Sample U_3 contains 6.48wt% K_2O (6g K_2O) surplus to the composition and CaF_2 has been completely omitted from the U_3 compound. As it can be seen in Fig.4, all samples U_1, U_2 and U_3 have a considerably higher viscosity as compared to molten reference powder (MRP). In case of ion-

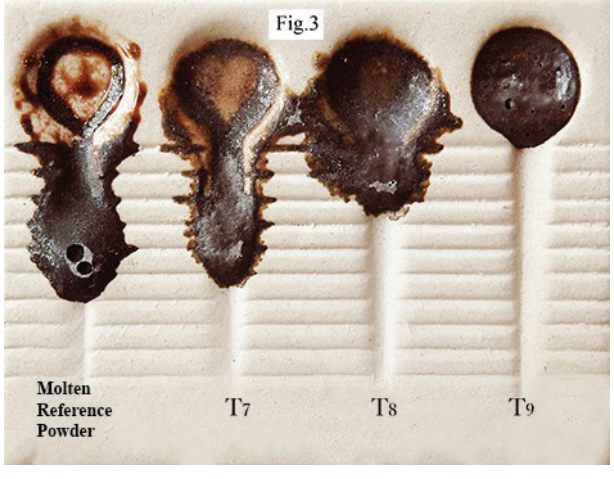

Fig.3. Schematic of molten samples of reference powder, T_7, T_8 and T_9 on the grooves of the groove viscometer.

ic exchange with each of the ions present in oxides of the mould powder (MP), K_2O an oxide with a big metallic ion (K^+) leads to higher viscosity. For example, if K_2O with either Na_2O or CaO or MgO replaces CaF_2 in the chemical composition of MP, the molten surface energy will grow due to the large size of the ion. (i.e. molten on the groove viscometer) (Fig.4). As a result, the tendency toward becoming spherical grows and hence, it prevents the molten surface area to extend. Fig.4 is a reason for this claim.

It can be concluded that the K_2O composition alone cannot be an appropriate substitute for CaF_2 in the MP's chemical composition.

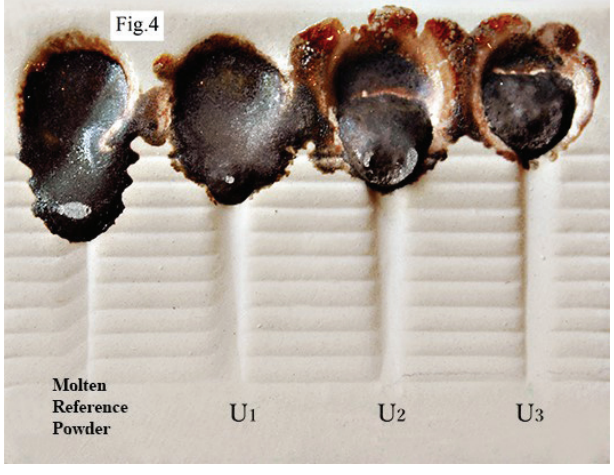

Fig.4. Schematic of molten samples of reference powder, U_1, U_2 and U_3 on the grooves of the groove viscometer.

3.1.4. Studying a combination of TiO_2, K_2O, Li_2O, ZnO and B_2O_3 on low-CaF_2 samples containing Portland Cement Clinker

Sample S_1 contained 1.04wt% F^-, 5.23wt% TiO_2, 0.42wt% Li_2O and 1.39wt% K_2O. With respect to Fig.5, sample S_1 shows a lower viscosity relative to that of the molten reference powder (MRP). Sample S_2 contained 1.04wt% F^-, 5.2wt% TiO_2, and 2.08wt% ZnO. According to Fig.5, sample S_2 reveals a partially similar viscosity compared with MRP. Sample S_3 contained 1.04wt% F^-, 5.2wt% TiO_2 and 2.08wt% B_2O_3. The sample too, has a viscosity rather similar to MRP and is also a good lubricant. (Fig.5). Samples S_1, S_2 and S_3, the F^- amount was constant in all samples which equalled 1.04wt%. Similarly, the TiO_2 level was constant in samples S_1, S_2 and S_3 and was determined to be 5.2wt%. It can be argued that the lubrication power of K_2O along with Li_2O (sample S_1) is higher than B_2O_3 (sample S_3) and the lubrication power of B_2O_3 is more than that of ZnO (sample S_2).

Fig.5. Schematic of molten samples of reference powder, S_1, S_2 and S_3 on the grooves of the groove viscometer.

Relation No. 5 depicts the lubrication power of the Li_2O, K_2O, B_2O_3 and ZnO oxides.

$$K_2O+Li_2O > B_2O_3 > ZnO \qquad \text{Eq. (5)}$$

It is worth mentioning that the presence of CaF_2, even in low quantities in samples S_1, S_2 and S_3 has played a crucial role in controlling the lubrication quality. On the other hand, it can be interpreted that in sample S_1, TiO_2, beside K_2O and Li_2O, has functioned as a glass maker. In other words, in sample S_1, the blend of CaF_2, TiO_2, K_2O and Li_2O is a noticeable combination which has directed the presence of 5.2wt% TiO_2 toward glass making. After replacing K_2O and Li_2O with ZnO in sample S_2, the lubrication or fluidity tended to decrease. In the sample, TiO_2 plays the role of a crystal-making agent. In sample S_3, similar to sample S_2, TiO_2 as a crystallizer alongside B_2O_3 established a higher viscosity than that of sample S_1, similar to sample S_2, and rather similar to the viscosity of MRP (Fig.5). Therefore, on using a combination of TiO_2, B_2O_3, and ZnO with a minimum amount of 1wt% F^-, a laboratory-scale of MP with a viscosity similar to that of MRP (molten reference powder) can be prepared.

3.2. Studying the crystallization of the samples

3.2.1. XRD phase

The XRF elemental analysis was conducted on the reference powder, the result of which is presented in Table 1.

XRD pattern of the reference powder is displayed in Fig.6. XRD pattern of the reference powder revealed such phases as wollastonite ($CaSiO_3$), silica (SiO_2), fluorine (CaF_2), corundum (Al_2O_3), manganese silicate ($MnSiO_3$), sodium carbonate (Na_2CO_3), CaMg (SiO_3)$_2$ and $CaAl_2O_4$. According to the pattern (Fig.6), the wollastonite phase

has the sharpest peak. It can be concluded that the base composition of this powder is CaO and SiO_2. Considering the fact, Portland Cement Clinker, which mainly consisted of CaO and SiO_2 and possesses the lowest amount of harmful sulfate impurities, was employed as the base component in preparing the MP's laboratory samples. In addition, according to the quantitative phase analysis of multi-phase system, the relation No.6 appears as follows[20]:

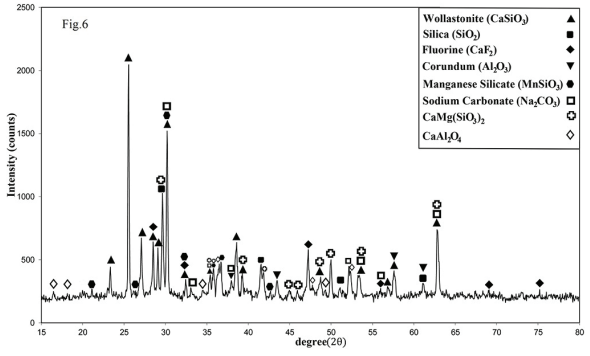

Fig.6. XRD pattern of the reference powder.

$$I_{eij}=K_{ei}.(X_{ij}/\mu_j^*) \quad \text{Eq. (6)}$$

Where I_{eij} is the diffracted intensity from the peak of phase "i" in sample "j", which is the area under the specified peak. The intensity can be obtained from the height multiplied to full width at the half maximum or β. K_{ei} is a constant related to the selected peak and nature of phase, geometry and electronic condition of an X-ray instrument, such as voltage, current, step size, time per step, etc. K_{ei} does not change with the weight fraction of phase "i" (X_{ij}). μ_j^* is the mass absorption coefficient of sample "j" which can be given as:

$$\mu_j^* = \sum_{n=1}^{p} \mu_n^* . X_n \quad \text{Eq. (7)}$$

While μ_n^* is the mass absorption coefficient of any of the elements "n" with a weight fraction of X_n inside the sample "j".

When the sample is fried to a high temperature, the elements do not necessarily change and only some loss on ignition occurs due to volatile materials.

We can trace any available phases remaining in the tempered sample. Fig.7 shows the XRD analysis of the MRP. It can be observed that all the phases have been transformed into new ones. Fluorine (CaF_2) has reacted with some phases and the overall phase changes are reviewed beneath:

$$Al_2O_3+2CaSiO_3=Al_2Ca_2SiO_7+SiO_2 \text{ (Glass)} \quad \text{Eq. (8)}$$

$$CaF_2+3CaSiO_3=Ca_4F_2Si_2O_7+SiO_2 \text{ (Glass)} \quad \text{Eq. (9)}$$

$$Na_2CO_3+Al_2O_3+2SiO_2=2NaAlSiO_4+CO_2 \quad \text{Eq. (10)}$$

$$CaMg(SiO_3)_2+CaSiO_3=Ca_2MgSi_2O_7+SiO_2 \text{ (Glass)} \quad \text{Eq. (11)}$$

$$CaAl_2O_4+CaSiO_3=CaAl_2SiO_7 \quad \text{Eq. (12)}$$

And the following equation illustrates the valence changes of manganese and formation of Mn_3O_4:

$$3MnSiO_3=3MnO+3SiO_2 \text{ (Glass)} \quad \text{Eq. (13)}$$

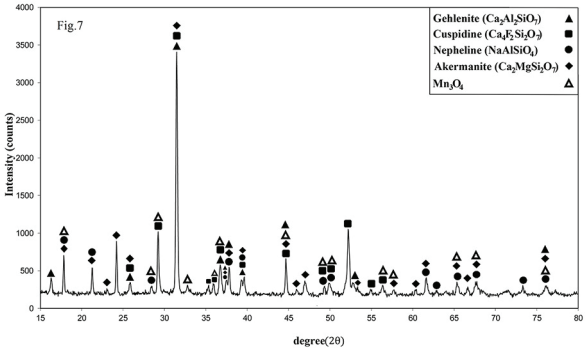

Fig.7. XRD pattern of the molten reference powder.

$$2MnO+1/2O_2=Mn_2O_3 \quad \text{Eq. (14)}$$

$$MnO+Mn_2O_3=Mn_3O_4 \quad \text{Eq. (15)}$$

In sample S_2, which is a combination of TiO_2 and ZnO and the raw materials with lower amounts of CaF_2, cause the following new reactions to occur (Fig.8):

$$TiO_2+CaSiO_3=CaTiO_3+SiO_2 \text{ (Glass)} \quad \text{Eq. (16)}$$

$$ZnO+Na_2CO_3+SiO_2=Na_2ZnSiO_4+CO_2 \quad \text{Eq. (17)}$$

With regard to this fact, the amount of CaF_2 has been reduced in order to diminish the hazardous effects of CaF_2 at high temperatures. Notably, the viscosity is almost similar to that of the molten reference powder.

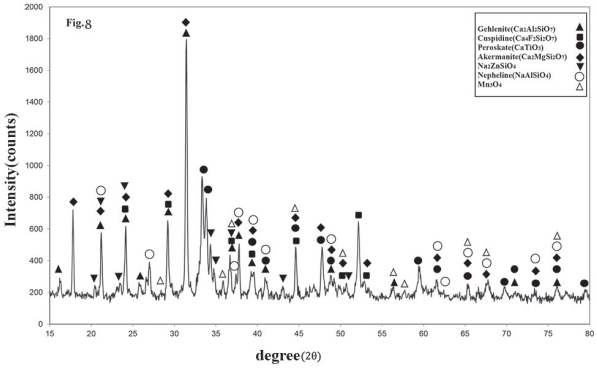

Fig.8. XRD pattern of sample S_2.

The outcome is a success in reducing CaF_2. The presence of Na_2CO_3 has been profitable in keeping the viscosity almost untouched. TiO_2 can be considered as a nucleating agent in the production of provskite ($CaTiO_3$) structure as well.

Sample S_3, CaF_2 is reduced and TiO_2 and B_2O_3 were added. Some phases were the same as those for MRP, namely as gehlenite ($Ca_2Al_2SiO_7$), cuspidine ($Ca_4F_2Si_2O_7$), nepheline ($NaAlSiO_4$), akermanite ($Ca_2MgSi_2O_7$) and Mn_3O_4. The two new phases are perovskite ($CaTiO_3$) and B_2SiO_5. The phase perovskite is explained beneath in which B_2O_3 has reacted as (Fig.9):

$$B_2O_3+SiO_2=B_2SiO_5 \qquad \text{Eq. (18)}$$

3.2.2. Microstructure

The research, SEM images at 1000x, 9000x and 16000x of the molten reference powder, samples S_2 and S_3 were prepared.

SEM images of MRP indicate the generation of crystals in the glass matrix. In other words, SEM images of the molten reference powder displays the molten with an expanded matrix which is a result of glass making.

During the solidification process, via glass saturation white crystalline particles are developed in the glass matrix. The event results in optimum viscosity for the molten reference powder (MRP) which is represented in Fig.10 (a) and 10 (b).

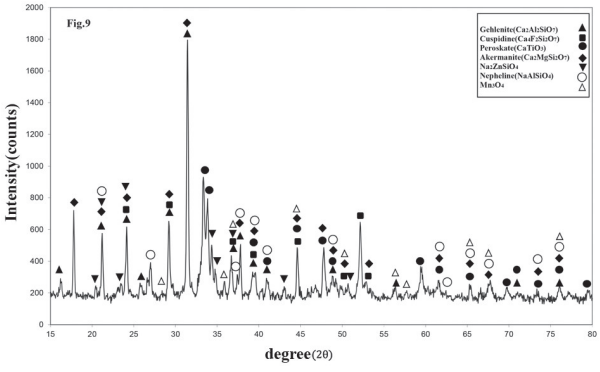

Fig.9. XRD pattern of sample S_3.

Fig.10(a)

Fig.10(b)

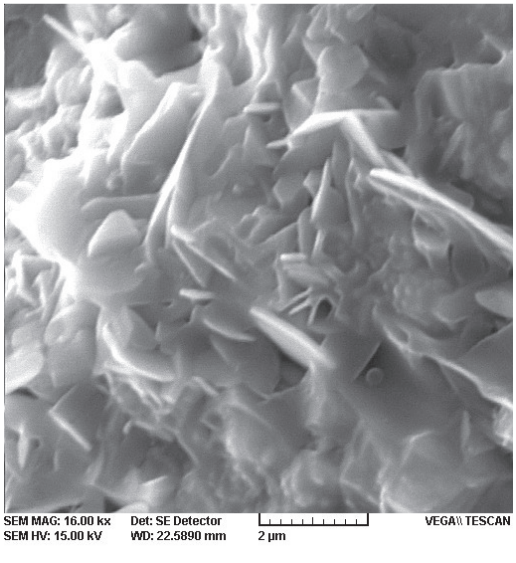

Fig.10. SEM images of the molten reference powder at a) 1000x and b) 16000x In a similar trend to MRP, SEM images of samples S2 and S3 (Fig.11 and 12, respectively), reveal the development of crystalline particles in the glass matrix.

.

Fig.11(a)

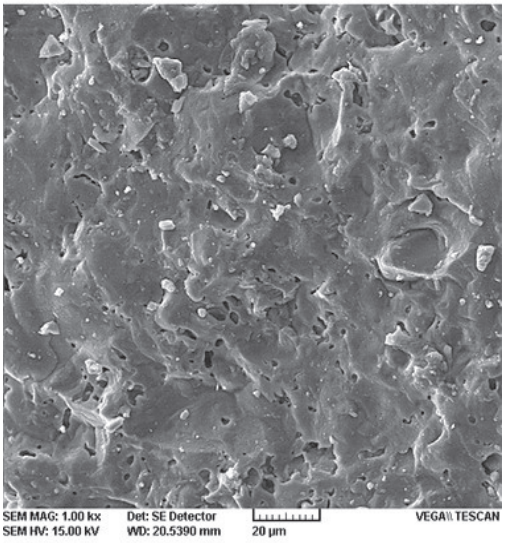

Fig.11(b)

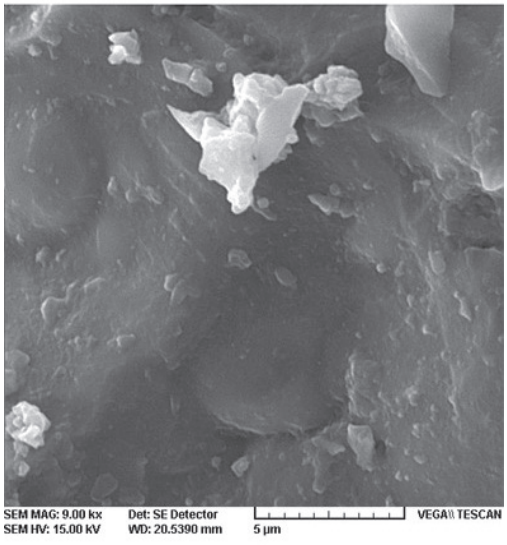

Fig.11(c)

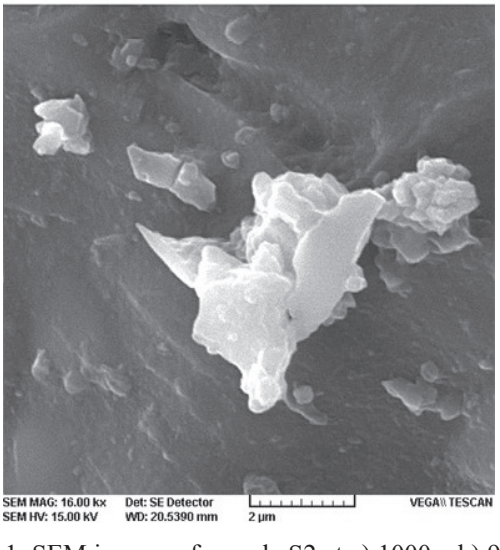

Fig.11. SEM images of sample S2 at a) 1000x, b) 9000x and c) 16000x.

Fig.12(a)

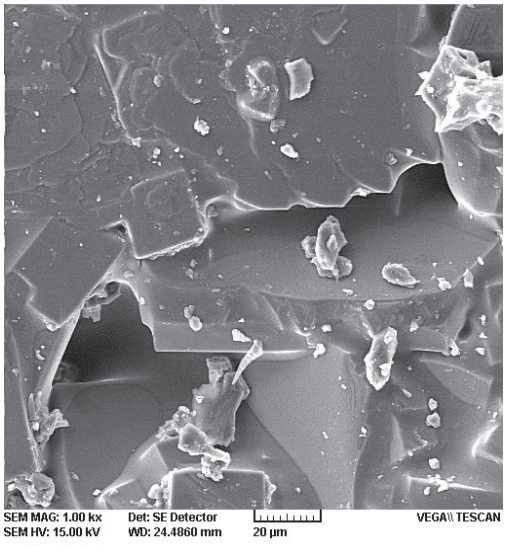

Fig.12(b)

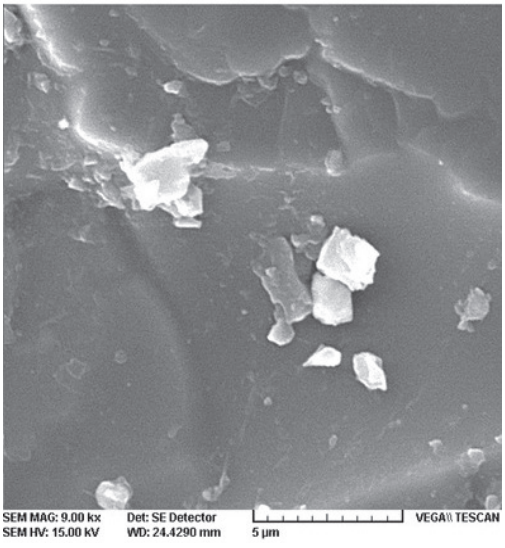

Fig.12(c)

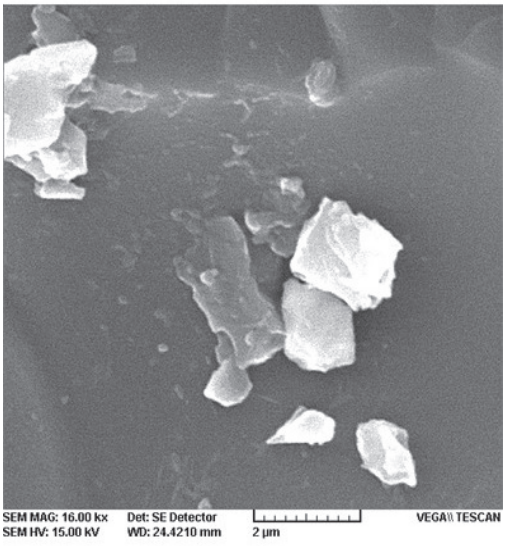

Fig.12. SEM images of sample S3 at a) 1000x, b) 9000x and c) 16000x.

With respect to their similarity of SEM images (Fig.11 and 12) with MRP (Fig.10), it can be concluded that all samples possess similar optimized viscosities compared with one another owing to their developing crystalline particles .

3.2.3. STA graph

To determine the melting and crystallization temperatures of the reference powder and sample S_2, STA (TGA/DTA) was carried out.

The TGA graph of the reference powder from 200°C to 1200°C proved a continuous decline of weight due to CO_2 gas emission and/or burning of carbon(c). Since carbon is an independent element and does not have wettability, it leaves the system in the form of gas (Fig.13). In other words, carbon lacks covalent bond (C-C) with any of the oxides (Fig.13).

Fig.13

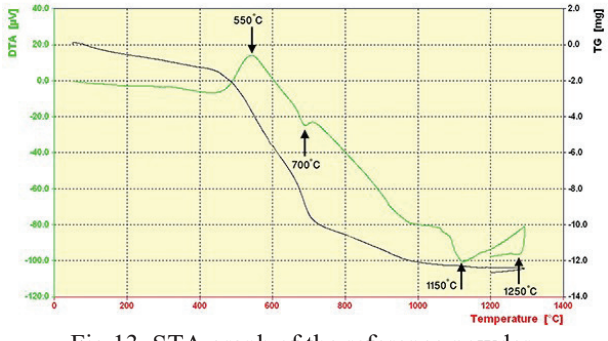

Fig.13. STA graph of the reference powder.

The DTA graph of the reference powder while being heated demonstrated an exothermic peak at about 550°C due to burning of carbon components. An endothermic peak was also observed at 700°C owing to the release of CO_2 and CO gases (Fig.13). Similarly, at the temperature of 1150°C, another endothermic peak was observed presenting the melting point of reference powder. In other words, at 1150°C the whole sample melted down. By reaching the temperature of 1250°C, the cooling procedure was carried out, during which the DTA graph of the reference powder reflected an endothermic peak. The peak is actually the crystallization temperature of the reference powder. The temperature is the threshold of crystallization in which an optimum viscosity for the reference powder is achieved.

As for the reference powder, around 200°C, the TGA graph of sample S_2 displays CO_2 gas emission which is evidently accompanied by weight loss. It stopped around 1200°C since in this sample less carbonate has been used and the required elements have been provided using the Portland cement clinker. In fact, it can be considered as a positive point in continuous casting of steel and reduces the amount of CO_2 gas emission to a minimum level (Fig.14).

Fig.14

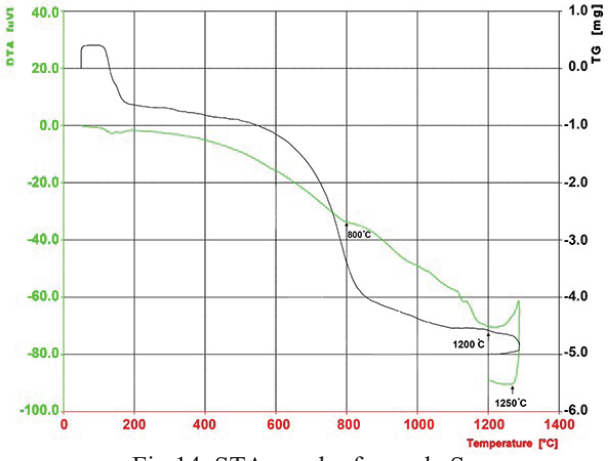

Fig.14. STA graph of sample S_2.

By the TGA graph can be defined for the heat loss as follows (Relation 19):

$$\text{Loss on ignition (LOI)} = \frac{|a\ amount\ of\ weight\ loss\ (mg)|}{Total\ sample\ weight\ (mg)} \times 100 \qquad \text{Eq. (19)}$$

With regard to the heat loss relation (Relation 19), the amount of weight loss in sample S_2 was 3.9 mg and the total sample weight was 48.34 mg (Fig.14) while the heat loss in sample S_2 has been 8.07 which is considerably lower than that of the reference powder (Table 1).

The DTA graph of sample S_2 (Fig.14) during heating showed no peak for burning carbon. Around the temperature of 800°C, however, a small endothermic peak appeared which signifies the emission of CO_2 gas. At about 1200°C, another endothermic peak was revealed which is the melting temperature for sample S_2. The peak resembles the reference powder's melting temperature obtained from its DTA graph (Fig.13). During the cooling process of the sample around 1250°C, an endothermic peak was observed that the peak is the crystallization temperature for sample S_2. The peak is similar to that of the reference powder as well (Fig.13).

4. Conclusions

- MgO is a refractory substance with a melting point of 2800oC which increases the viscosity of the mould powder. In other words, MgO alongside SiO_2 form forsterite in the chemical composition of the mould powder. Forsterite, with a melting point of 1890oC, reduces the fluidity of the mould powder and enhances its viscosity.
  Li_2O in amounts lower than 0.22wt% acts as bond-breaking composition in the chemical composition of mould powders (MP) and decreases their viscosity. Employing Li2O in amounts higher than 0.22wt% acts as a glass-making composition in the

chemical composition of mould powders and enhances their viscosity.

- K_2O is an oxide containing K^+, which is a large metal ion. If K^+ possesses ionic transfer with any of the present ions in oxides of the mould powders, the surface energy of the molten powder will be incremented due to the largeness of the metal ion. As a result, the molten powder highly tends to become spherical. These two factors on one hand, prevent from the expansion of the molten powder, the increase of its fluidity and an optimum lubrication, while on the other, develops its viscosity.
- Using TiO_2 in amounts lower than 6wt% and utilizing components such as ZnO and B_2O_3, two low-CaF_2 samples were prepared. TiO_2 in these two samples forms the crystalline phase of perovskite, which results in nucleation in the chemical composition of the mould powder. The phase functions as the crystalline phase of cuspidine which results in optimizing the viscosity of the mould powder. These two samples, for the first time, are two ideal low-CaF_2 mould powder samples regarding their similarity in viscosity and crystallization to those of the reference powder, which can be apt substitutions for the reference powder in laboratory scales.
- The research, a low-CaF_2 sample containing Portland Cement Clinker, TiO_2, CaF_2 and ZnO was prepared having a much lower loss on ignition in comparison with the reference powder. In addition, the DTA graph of the sample revealed a similarity between the melting and crystallization temperatures of this sample with those of the reference powder.
- Considering the TGA graph of the low-CaF_2 sample, noted in conclusion No.5, and its lower loss on ignition in comparison to the reference powder as well as regarding the XRD pattern of the reference powder showing $CaSiO_3$ as its highest peak, it can be concluded that Portland Cement Clinker can be applied as the base component of mould powders instead of high-purified wollastonite which is rare as well as being blast furnace slag with having some impurities.

Reference

[1] A.B. Fox, K.C. Mills., D. Lever, M.C. Bezerra, C. Valadares, I. Inamuno, J.J. Laraudogoitia and J.Gisby: J. ISIJ Int., 45(2005), 1051-1058.

[2] K.C. Mills, A.B. Fox, R.P. Thackray and Z. Li: Proceeding of 7th International Conference on Molten Slags Fluxes and Salts, The South African Institute of Mining and Metallurgy, (2004).

[3] A. Kondratiev, P.C. Hayes and E. Jak: J. ISIJ. Int., 46 (2006), 375-384.

[4] P. Scheller: Proceeding of VII International Conference on Molten Slags Fluxes and Salts, The South African Institute of Mining and Metallurgy, (2004), 411-415.

[5] W. Wang, K. Blazek and A. Cramb: J. Metall. and Mat. Trans. B., 39B(2008), 66-74.

[6] A. Kondratiev, P.C. Hayes and E. Jak: J. ISIJ Int., 46(2006), 368-374.

[7] A. Nowak and R.A. Bialecki: Institute of Fluid Mechanics and Heat Transfer EUROTHERM 82, Gliwice-Cracow, (2005).

[8] G. Wen, S. Sridhar, P. Tang, X. Qi and Y. Liu: J. ISIJ. Int., 47(2007), 1117-1125.

[9] S.Y. Choi, D.H. Lee, D.W. Shin, J.W. Cho and J.M. Park: J. Non-Crys. Sol., 345&346(2004), 157-160.

[10] X. Qi, G.H. Wen, and P. Tang: J.Non-Crys. Sol., 354(2008), 5444-5452.

[11] C.A. Pinherio, I.V. Samarasekera, J.K. Brimacombe: J. Iron. And Steel., (2004). 56-60.

[12] J.Y. Chung: J. Mat.s Sci. For., 561(2007), 3-4.

[13] M. Nakamoto, Y. Miyabayashi, L. Holappa and T. Tanaka: J. ISIJ. Int., 47(2007), 1409-1415.

[14] M. Mueller, W. Willenborg, K. Hilpert and L. Singheiser: VII International Conference on molten slage, fluxes and salts, The South African Institute of Minig and Metallurgy, (2004).

[15] M. Nakamoto, J. Lee and T. Tanaka: J. ISIJ. Int., 45(2005), 651-656.

[16] R.F. Brooks, A.T. Dinsdale and P.N. Quested: J. Meas. Sci. Technol., 16 (2005), 354-362.

[17] Q. Shu and J. Zhang: J. Uni. Sci. and Tech. Bei., 12 (2005), 221.

[18] A. Kondratiev, P.C. Hayes and E. Jak: J. ISIJ. Int., 46(2006), 359-367.

[19] W. En-fa, Y. Yin-dong, F. Chang-lin, I.D. Sommerville and A. McLean: J. Iron. And Steel. Res. Int., 13(2006), 22-26.

[20] A. Monshi and P.F. Messer: J. Mat. Sci., 26(1991), 3623-3627.